Chemical Engineering Journal 285 (2016): 228 - 235

DOI: http://dx.doi.org/10.1016/j.cej.2015.10.002

Deducing kinetic constants for the hydrodechlorination of 4-chlorophenol using high adsorption capacity catalysts

*Macarena Munoz[1], Malte Kaspereit[2] and Bastian J.M. Etzold[1]**

[1]Lehrstuhl für Chemische Reaktionstechnik
Friedrich-Alexander-Universität Erlangen-Nürnberg
91058 Erlangen, Germany
[2]Lehrstuhl für Thermische Verfahrenstechnik
Friedrich-Alexander-Universität Erlangen-Nürnberg
91058 Erlangen, Germany

*Corresponding author: Prof. Bastian J.M. Etzold
Tel.: +49 (9131) 85 - 27430
Fax: +49 (9131) 85 - 27421
E-mail: bastian.etzold@fau.de

Keywords: Catalytic hydrodechlorination; adsorption; kinetic model; 4-chlorophenol; Pd; activated carbon.

Abstract

Employing high surface area supports for catalytic hydrodechlorination can result in pronounced adsorption of reactants, intermediates and products. The influence of these sorption processes on the activity and selectivity upon 4-chlorophenol (4-CP) hydrodechlorination in aqueous solution has been studied using four commercial Pd/Al_2O_3 and Pd/AC catalysts at ambient pressure within the temperature range of 20-40 °C ($[4\text{-CP}]_0$ = 0.78 – 2.90 mmol L^{-1}, [catalyst] = 1 g L^{-1}, 50 NmL H_2 min^{-1}). The adsorption capacity of the catalysts was independently evaluated. The Al_2O_3-based catalyst did not show any significant adsorption of those species whereas the activated carbon materials presented in all cases high uptakes (e.g. up to 2.4 $mmol_{4\text{-CP}}$ g_{cat}^{-1}). In order to deduce true kinetic constants also for these catalysts, a kinetic model was developed, which accounts for the consecutive reaction and sorption processes in parallel. This expanded model resulted in a reasonable fit, can thus be used for comparison of different catalysts regardless their sorption capacity and allows predicting successfully the selectivity to the reaction products.

1. Introduction

The increasing social and political concern on environment demands a more rigorous control of industrial wastewaters and thus, the development and implementation of new technologies capable to deal with toxic pollutants resistant to the broadly established conventional methods. Among these hazardous pollutants, chlorophenols (CPs) require special attention due to their high toxicity, persistence and low biodegradability. Because of their antimicrobial properties, they are commercially important chemicals with an estimated production of ca. 100 kt per year (Pera-Titus et al., 2004), being widely used in a diversity of industrial processes related to the manufacture of pesticides, pharmaceuticals, dyes and wood preservatives. As a result, they have been detected in both surface and ground waters [1-4], which involves a significant risk for the environment.

Catalytic hydrodechlorination (HDC) appears as a promising technology for the treatment of wastewater containing organochlorinated pollutants since it shows remarkable advantages when compared to other techniques [5-7]. HDC can operate at mild conditions, not requiring high temperatures and/or pressures as in the case of incineration or wet oxidation processes. Large amounts of reagents, such as in Fenton oxidation, are not needed. It is also efficient within a wide range of concentrations of chlorinated compounds, which is not the case of biological methods. Furthermore, in contrast to oxidation processes, HDC is not strongly affected by the number of atoms of the pollutant [8]. In this process the organochlorinated compound reacts with hydrogen leading to the formation of hydrogen chloride and hydrocarbons. Although HDC does not provide the complete destruction of the pollutants, it leads to their convenient transformation into substantially less harmful species, which involves a significant decrease on the ecotoxicity of the effluent [6]. Accordingly, HDC has been regarded as a detoxifying stage prior to oxidation [8, 9] or biological treatments [10]. Nevertheless, from an economic point of view, the formation of valuable non-chlorinated hydrocarbons could be also a potential advantage since they may be reused as raw material, as it is the case of phenol, an important industrial precursor to many materials and useful compounds [11]. On the other hand, the main

drawback of this technology, which has limited so far its widespread application, is the relatively low stability of the catalysts due to chloride poisoning (Diaz et al., 2011).

HDC reactions have been studied over a number of metals, being those based on Pd [6, 12-17], Pt [14, 17] and Rh [14, 17-19] with metal loadings ranging from 0.5 to 10% (w/w) the most active ones. Among them, Pd is the metal least affected by the catalyst poisoning properties of the chloride ions released [20, 21] and is commonly identified as the most suitable active phase for liquid-phase HDC [20, 22]. The catalytic support plays also an important role in both catalytic activity and stability and has been investigated on carbon [6, 23-25], alumina [14, 16, 26], zirconia [27, 28] and pillared clays [29, 30], among other, with alumina and activated carbon being the most reported systems in the literature [15, 31, 32]. It is generally accepted that alumina presents a high mechanical resistance and a strong interaction with supported metals leading to enhanced metal dispersion but it is also quite sensitive to the HCl formed upon the reaction [20, 33]. In contrast, activated carbon is relatively inert to the HCl generated and has been postulated as very suitable support for HDC [20]. Moreover, depending on the catalytic requirements the carbon porosity and surface chemistry can be tuned through the manufacturing and activation processes [23, 34].

The reaction mechanism of chlorophenols hydrodechlorination has been widely studied in the literature [14, 16, 17, 26, 35-38]. It is generally accepted that monochlorophenols react with hydrogen to produce phenol (Ph), which is further hydrogenated to cyclohexanone (C-one) [17, 26, 36-38]. Cyclohexanol (C-ol) can also be formed by hydrogenation of C-one when Rh or Pt are used as active phase [17, 26, 36] or when activated carbon-supported-Pd catalysts containing high amounts of oxygen surface groups, especially carboxylic acids and lactones, are employed [23]. The experiments of those studies are normally described by simple pseudo-first order rate equations, where the H_2 and catalyst concentration are included in the kinetic constants [14, 17, 26]. For simplicity the few kinetic studies reported in the literature do not consider the contribution of the adsorption of the pollutant as well as the intermediates onto the support, although it can be highly pronounced when carbon-based catalysts are used. The commonly applied procedure to obtain similar starting reaction conditions for catalysts with

different adsorption capacity is to pre-adsorb the reactant onto the catalyst [23, 39]. However, this oversimplification is problematic at strong adsorption since it does not allow closing the mass balance. Thus, the kinetic constants deduced cannot be used for comparison of different catalysts or to estimate the performance at technical scale. Schindler et al. [13] made a first attempt to account for the adsorption of HDC of 4-chlorophenol (4-CP). The work is restricted to the initial stage of adsorption and reaction on one activated carbon fibre supported catalyst.

In this study we compare two kinetic models for HDC of 4-CP, which neglect or account, for the sorption of the reactant 4-CP, the product Ph and the consecutive product C-one. The models are applied to describe experimental data derived from four different commercial Pd/Al_2O_3 and Pd/AC catalysts for the full course of reaction and to deduce the rate constants as a measure for the activity, while only the model accounting for the sorption steps results in a reasonable fit. Finally the kinetic data is used to simulate the course of reaction and selectivity towards the intermediate product Ph, which is strongly affected by ad/desorption on the catalyst support and is not directly available from the free phase concentration measured during the experiments.

2. Materials and methods

2.1. Catalysts

Commercial catalysts were delivered by Alfa Aesar (AA) and Sigma Aldrich (SA) and were dried before use to remove physisorbed water. The alumina-based catalyst presents 1 wt.% Pd whereas the carbon-supported ones contain 1, 5 and 10 wt.% Pd according to the specification. Correspondingly, the catalysts have been denoted as Pd/Al_2O_3, Pd/AC-AA(1), Pd/AC-SA(5) and Pd/AC-AA(10).

2.2. Catalyst characterization

The porous structure of the catalysts was characterized from nitrogen adsorption-desorption at -196 °C using a Micromeritics ASAP 2010 apparatus. The samples were previously degassed overnight at

150 °C. The particle size of the catalysts was measured in aqueous suspensions by dynamic light scattering using a Mastersizer 2000 system (Malvern Instruments).

2.3. Typical reaction procedure

The aqueous phase HDC runs were performed in a glass slurry-type reactor (250 mL) where hydrogen was continuously fed at 50 NmL min^{-1}. A reaction volume of 150 mL, a catalyst concentration of 1 g L^{-1} and a stirring velocity of 750 rpm were always used, whereas the temperature was investigated within the 20-40 ºC range. The starting concentration of 4-CP was fixed at 0.78 mmol L^{-1} and 2.90 mmol L^{-1} for Pd-supported on alumina and AC catalysts, respectively. 0.78 mmol L^{-1} was selected as it is a representative concentration of chlorophenols in several industrial wastewaters (e.g. chlorine pulp bleaching, manufacture of pesticides, pharmaceuticals and paints, among other) (Maloney et al., 1986; Ghaly et al., 2001). The higher concentration used with the AC catalysts is due to the high adsorption capacity of those supports. Blank tests intended to confirm that the reaction did not proceed in the absence of catalyst were conducted at all the temperatures tested. The existence of both internal and external mass transfer limitations in the experiments was found to be negligible from the values of the Carberry and Weisz-Prater numbers (see Tables S1 and S2 in Supplementary Material). Model simulations were undertaken using the kinetic modelling software package Presto-kinetics version 7.2.2.

The equilibrium adsorption tests with AC-based catalysts were carried out under the same operating conditions and procedure as the HDC tests but in the absence of hydrogen. In this case, 4-CP, Ph and C-one solutions were prepared with concentrations from 0 to 10 mmol L^{-1}. The equilibration time was 1 h for all the samples. The equilibration data were analysed using the Langmuir equation expressing the relation between the adsorbed amount per unit adsorbent mass and the concentration in solution (Eq. 1).

$$C_{ADS_i} = \frac{K_{SORP_i} \cdot C_{ADS-MAX_i} \cdot C_{FREE}}{1 + K_{SORP_i} \cdot C_{FREE}} \quad (1)$$

i = 4-CP, Ph, C-one.

where C_{ADS} is the amount of solute adsorbed on the solid catalyst at equilibrium; C_{FREE} is the equilibrium concentration of solute in solution; K_{SORP} is the Langmuir adsorption equilibrium constant and $C_{ADS-MAX}$ is the maximum possible amount of solute adsorbed per unit mass of catalyst.

The progress of the HDC and/or adsorption runs was followed by periodically withdrawing and analyzing liquid samples from the reactor. The catalyst was separated by filtration using a PTFE filter (pore size 0.2 μm). 4-CP, Ph and C-one were analyzed by GC/FID (3900, Varian) using a 25 m length and 0.32 mm i.d. capillary column (CP-FFAP CB, Varian) and nitrogen as carrier gas (30 mLN min^{-1}). The temperatures at the injector and FID detector were set at 150 and 300 ºC, respectively. The temperature in the column was increased from 70 to 240 ºC at a constant ramp of 15 ºC min^{-1}, allowing the proper separation of 4-CP, Ph and C-one at retention times of 11.2, 8.6 and 4.2 min, respectively. Chloride was analysed using an IC25 Ion Chromatograph equipped with a 2x250mm IonPak AG11-HC column and a 2x50mm AS11-HC pre-column (Dionex). The hydroxide eluent was provided by an EGC III KOH eluent generator cartridge. Flow rate and sample volume were 0.4 mL/min and 100ul, respectively.

3. Results and discussion

3.1. Evaluation of the adsorption capacity of the catalysts

The catalysts studied differ strongly in their pore structure and surface composition. The alumina catalyst shows approximately a 3 times lower specific surface area and 2 times lower pore volume compared to the activated carbons (for more details on characterization results see Supplementary Material). The influence of these differences on the adsorption of compounds from the reaction mixture was studied within the relevant concentration range where HDC experiments were carried out. The effect of temperature on the adsorption capacity of the catalysts was also evaluated with Pd/Al_2O_3 and

Pd/AC-AA(1) within the range of 20-40 °C. Independent adsorption equilibrium experiments, without parallel reactions, were ensured by the absence of H_2. All AC-based materials showed a high uptake for all species. As representative example, Fig. 1 depicts the obtained adsorption isotherms at 30 °C with Pd/AC-AA(1) (the other isotherms are given in the Supplementary Material). For Pd/Al_2O_3 only negligible uptake resulted. Hence, not only a 3 times lower uptake, which could have been explained by the lower specific surface area is observed but a more or less complete absence of adsorption. The difference in surface interaction with the hydrophilic metal oxide surface compared to the hydrophobic carbon one should be the major reason for this observation. For the AC materials the Langmuir isotherm was applied to fit the experimental sorption results and obtain adsorption equilibrium constant (K_{SORP}) and maximum compound uptake per unit adsorbent mass ($C_{ADS-MAX}$). Table 1 compares the data obtained for the different AC-based catalysts at 30 °C (for data at other temperatures see Supplementary Material). The results obtained are consistent with those previously reported in the literature for the adsorption of 4-CP and Ph using different activated carbons [40, 41]. Particularly, the K_{SORP} values obtained follow the same trend that those reported by Shindler et al. [13], who also found that $K_{SORP-4CP}$ can be up to 4 times higher than that of Ph. However, the $C_{ADS-MAX}$ values showed in that work are around 2 times higher (5.2 and 4.1 mmol g^{-1} for 4-CP and Ph, respectively) than those obtained in this work, which is consistent with the significantly higher surface area of their AC support (1460 m^2 g^{-1}).

3.2. Model set-up

The sorption study clearly demonstrates that for the AC-based catalysts pronounced sorption of all species in the reaction mixture takes place and thus, needs to be accounted, when deducing rate constants. To demonstrate the influence, in this work HDC experiments were carried out with the four catalysts differing strongly in their sorption characteristics and two kinetic models (compared in Scheme 1) were applied to describe the resulting concentration profiles and to deduce kinetic constants. To be

able to compare different palladium loadings, the modified reaction time t_{mod} was employed. It is defined as the product of time and concentration of Pd as follows:

$$t_{mod} = t\frac{m_{cat,Pd}}{V} \tag{2}$$

Model 1 is the one mainly used in literature and, as shown in Scheme 1, only accounts for the consecutive reaction network, while ignoring the sorption processes. Considering that the process takes place under kinetic control and that the amount of Pd as also the hydrogen pressure is kept constant during the experiments, pseudo-first order kinetics with regard to the organic reactants can be applied [14, 17, 26]:

$$\frac{dC_{4-CP}}{dt_{mod}} = -k_{HDC-1} \cdot C_{4-CP} \tag{3}$$

$$\frac{dC_{Ph}}{dt_{mod}} = k_{HDC-1} \cdot C_{4-CP} - k_{HDC-2} \cdot C_{Ph} \tag{4}$$

$$\frac{dC_{C-one}}{dt_{mod}} = k_{HDC-2} \cdot C_{Ph} \tag{5}$$

Model 2 additionally accounts for all ad- and desorption processes of the three compounds involved. Further assumptions are that the adsorption takes place onto active carbon and not on Pd (Shindler et al., 2001; Diaz et al., 2011). Additionally surface diffusion of adsorbed species towards reactive sites is ignored. In this model the same pseudo-first order approaches are used for the consecutive reaction steps. The parallel sorption processes are implemented according to the Langmuir assumptions (total number of free and occupied sorption sites is constant; adsorption: first order with regard to the amount of free sites and concentration of adsorbate in solution; desorption: first order with regard to adsorbed species concentration). Based on this the net production rates of the compounds involved in the overall reaction can be expressed with Eqs. (6)-(12):

$$\frac{C_{4-CP\,FREE}}{dt_{mod}} = -k_{HDC-1} \cdot C_{4-CP\,FREE} - k_{ADS-1} \cdot C_{4-CP\,FREE} \cdot L + \frac{k_{ADS-1} \cdot C_{4-CP\,ADS}}{K_{SORP-4-CP}} \tag{6}$$

$$\frac{dC_{4-CP\ ADS}}{dt_{mod}} = k_{ADS-1} \cdot C_{4-CP\ FREE} \cdot L - \frac{k_{ADS-1} \cdot C_{4-CP\ ADS}}{K_{SORP-4-CP}} \quad (7)$$

$$\frac{dL}{dt_{mod}} = -k_{ADS-1} \cdot C_{4-CP\ FREE} \cdot L + \frac{k_{ADS-1} \cdot C_{4-CP\ ADS}}{K_{SORP-4-CP}} - k_{ADS-2} \cdot C_{Ph\ FREE} \cdot L + \frac{k_{ADS-2} \cdot C_{Ph\ ADS}}{K_{SORP-Ph}} - k_{ADS-3} \cdot C_{C-one\ FREE} \cdot L + \frac{k_{ADS-3} \cdot C_{C-one\ ADS}}{K_{SORP-C-one}} \quad (8)$$

$$\frac{dC_{Ph\ FREE}}{dt_{mod}} = k_{HDC-1} \cdot C_{4-CP\ FREE} - k_{HDC-2} \cdot C_{Ph\ FREE} - k_{ADS-2} \cdot C_{Ph\ FREE} \cdot L + \frac{k_{ADS-2} \cdot C_{Ph\ ADS}}{K_{SORP-Ph}} \quad (9)$$

$$\frac{dC_{Ph\ ADS}}{dt_{mod}} = k_{ADS-2} \cdot C_{Ph\ FREE} \cdot L - \frac{k_{ADS-2} \cdot C_{Ph\ ADS}}{K_{SORP-Ph}} \quad (10)$$

$$\frac{dC_{C-one\ FREE}}{dt_{mod}} = k_{HDC-2} \cdot C_{Ph\ FREE} - k_{ADS-3} \cdot C_{C-one\ FREE} \cdot L + \frac{k_{ADS-3} \cdot C_{-One\ ADS}}{K_{SORP-C-one}} \quad (11)$$

$$\frac{dC_{C-one\ ADS}}{dt_{mod}} = k_{ADS-3} \cdot C_{C-one\ FREE} \cdot L - \frac{k_{ADS-3} \cdot C_{C-one\ ADS}}{K_{SORP-C-one}} \quad (12)$$

where $C_{4\text{-CP FREE}}$, $C_{Ph\ FREE}$ and $C_{C\text{-one FREE}}$ are the concentrations of 4-CP, Ph and C-one free in solution; $C_{4\text{-CP ADS}}$, $C_{Ph\ ADS}$ and $C_{C\text{-one ADS}}$ are the concentrations of 4-CP, Ph and C-one adsorbed onto the AC support; $k_{HDC\text{-}1}$ and $k_{HDC\text{-}2}$ are the HDC apparent first order rate constants of each HDC reaction step shown in Scheme 1; $k_{ADS\text{-}1}$, $k_{ADS\text{-}2}$ and $k_{ADS\text{-}3}$ are the adsorption rate constants of 4-CP, Ph and C-one; $K_{SORP\text{-}1}$, $K_{SORP\text{-}2}$ and $K_{SORP\text{-}3}$ are the Langmuir adsorption equilibrium constants previously calculated in the adsorption equilibrium experiments for 4-CP, Ph and C-one; and L represents the amount of free sites present in the AC support, whose initial value corresponds to the maximum adsorbed concentration ($C_{ADS\text{-}MAX}$), also determined in the adsorption equilibrium experiments.

3.3. Model evaluation: HDC of 4-CP with Pd/Al_2O_3 and Pd/AC catalysts

To study the feasibility of the kinetic models for fitting experimental results and obtaining kinetic data, HDC experiments were carried out with the four different alumina and activated carbon supported catalysts employed already for the sorption study. When employing model 2, it was additionally

assumed that the sorption process is relatively fast compared to the reaction. Thus, all adsorption rate constants k_{ADS-1}, k_{ADS-2} and k_{ADS-3} were set to relatively high in comparison to the reaction rate constants (minimum factor 100) and only later on varied in the fitting procedure. Variation of the adsorption rate constants showed also that the model is insensitive to these parameters, corroborating the assumptions. The Carberry number and correlation of Hoffer et al. [42] were employed to ensure that the experiments were carried out in the intrinsic kinetic regime (see Supplementary Material).

In first place the results obtained at 30 °C with the extremely low adsorption capacity catalyst (Pd/Al_2O_3) and a high adsorption capacity one (Pd/AC-AA(1)) are compared. The concentration profiles resulting for the Pd/Al_2O_3 with negligible adsorption can be described in a good manner with both models (Fig. 2), obtaining the same HDC rate constants (Table 2). An additional indicator that no adsorption took place is the amount of chloride ions formed, which was determined by the pH and ion chromatography. Approximately all free 4-CP depleted from the solution led to chloride ion formation (balance closed to 95%), hence, underwent the HDC reaction. Thus, due to the negligible adsorption capacity of the Al_2O_3 support, the simplification of model 1 is unproblematic and both models are suitable to derive the kinetic rate constants.

However, when trying to simulate the concentration profiles resulting with Pd/AC-AA(1) as catalyst, model 1 did not lead to favourable results. The concentration of Ph predicted was around 1.7 mmol L^{-1} higher than the experimental one (Fig. 3a). On the opposite, as can be seen in Fig. 3b, model 2 allowed a fairly good fit of the experimental results. The rate constants derived with both models differ up to 27 % for k_{HDC-1} and 65 % for k_{HDC-2} (rate constants are given in Table 3).

Model 2 predicted that all free and adsorbed 4-CP was dechlorinated at the end of the experiment. To check this, the amount of produced chloride ions was measured and resulted to ≈2.8 mmol L^{-1}, which is 96% of chlorine added as 4-CP. Additionally, a desorption study of the spent catalyst was carried out, by introducing it into a basic solution (NaOH 1M) for 2 h [43-45]. Pronounced desorption of Ph could be

detected whereas 4-CP did not appear, corroborating the simulation. All in all, employing model 2 allowed closing the carbon balance during the whole reactions for 99% and the chloride ions at the end of the reactions above 95%.

Similarly, model 2 was capable of describing accurately the experimental results obtained at 20 and 40 °C with both catalysts (see Supplementary Material for Figures), while model 1 resulted in strong deviations to the experimental data when the high adsorption capacity catalyst was used. Tables 2 and 3 collect the kinetic constants determined with model 2 as well as the pH values obtained at the end of the reactions with Pd/Al_2O_3 and Pd/AC-AA(1) catalysts, respectively. The pH was strongly reduced from its initial value ($pH_0 \approx 6.0$) due to the formation of HCl upon 4-CP HDC. From the values of $k_{HDC\text{-}1}$ derived with model 2 and for different temperatures, the apparent activation energy for 4-CP hydrodechlorination has been calculated from the Arrhenius equation, obtaining values of 38 and 28 kJ mol^{-1} for Pd/Al_2O_3 and Pd/AC-AA(1) catalysts, respectively. Those results are consistent with previous works [13, 31]. Molina et al. [17] reported a value of 39 kJ mol^{-1} with Pd-supported on pillared clay within the range of 25 to 50 °C. Diaz et al. [14] gave 47 kJ mol^{-1} with commercial $Pd/\gamma\text{-}Al_2O_3$ within 20 to 40 °C and Shindler et al. [13] obtained a value of 25 kJ mol^{-1} in the temperature range 30-85 °C with a commercial Pd/AC catalyst.

Comparing both catalysts the rate constants $k_{HDC\text{-}1}$ were around 6 times higher at all the temperatures tested with the AC-based one. On the other hand, the activity for the consecutive hydrogenation of Ph was approx. 2 orders of magnitude lower than that of Pd/Al_2O_3, which is consistent with previous works dealing with Pd-supported catalysts [14, 17, 26]. However, it is important to highlight that the support presented a significant effect on consecutive hydrogenation and the difference of $k_{HDC\text{-}1}$ to $k_{HDC\text{-}2}$ increases to even 3 orders of magnitude for Pd/AC-AA(1). The high difference is of importance, if despite detoxification of 4-CP also Ph as intermediate shall be produced in high selectivity.

The same parameter fitting with both models was also carried out for the remaining two catalysts Pd/AC-SA(5) and Pd/AC-AA(10) at 30 °C. The obtained kinetic rate constants and the experimental

and predicted concentration curves have been included in the Supplementary Material. The parity plots in Fig. 4 finally compare the calculated and measured concentrations for all catalysts in the HDC of 4-CP at 30 °C. The high deviation of model 1 clearly shows that for high sorption capacity catalysts the kinetic data cannot be obtained like done often in literature, hence, with this oversimplified model 1 or even with a simple first order fit to the initial rate of depletion for 4-CP. Despite the wrong rate constants obtained, the amount of chloride ions formed will be calculated wrong and thus also the change of pH with the course of reaction.

3.4. Employing the determined kinetic data to simulate selectivity towards phenol

Model 2 and the kinetic data deduced for the different catalysts are finally employed to calculate the selectivity towards the intermediate Ph that can be obtained. From the batch experiments this data is not directly available as not all Ph is present in the solution but also adsorbed. Thus selectivity calculated directly from the solution concentration will be too low. Fig. 5 shows the calculated selectivity to Ph and C-one for all the catalysts. As has been aforementioned, the support plays an important role on the ratio of both reaction steps in the consecutive reaction network. With Pd/AC-AA(1) an extraordinary selectivity of 99% can be obtained at 99% of 4-CP conversion. Contrary, Pd/Al_2O_3 with a faster Ph hydrogenation activity shows a progressive decrease on the selectivity with increasing degree of conversion and at 99% of 4-CP conversion only a selectivity to Ph of 89% can be obtained. The other two AC supported catalysts with higher Pd loading are in between, and a trend for higher Ph selectivity with lower Pd loading results from the interplay of adsorption and reaction. Thus, depending if a process aims only at detoxification of organochlorinated compounds or also at production of chemicals from the intermediates obtained, a high or a low active metal loading on a high sorption capacity support is advantageous.

4. Conclusions

In this work, we have demonstrated that ad- and desorption of the target pollutant as well as the reaction products need to be taken into account to deduce true kinetic constants for the HDC process. It has been shown that the conventional kinetic model only allows fitting the experimental results when negligible adsorption capacity catalysts such as alumina are employed. However, when AC-based catalysts are used the HDC constants were always overestimated and the carbon balance could not be closed as more than 50% of the carbon was adsorbed onto the support. Including the sorption processes in the kinetic model resulted in a reasonable fit with both negligible and high adsorption capacity catalysts. Furthermore, it allowed closing the mass balance during the whole course of reaction and predicting accurately the selectivity to the reaction products. As true HDC kinetic constants are obtained, the comparison of different catalysts is possible as well as the estimation of their performance at technical scale.

As has been shown, the support plays an important role on both HDC and hydrogenation reaction steps in the consecutive reaction network. The application of AC-based catalysts has proved to be advantageous compared to alumina ones as in all cases higher HDC rates have been obtained. On the other hand, depending on the goal of the process the selectivity to the reaction products can be appropriately tuned by modifying the Pd loading.

Figure captions

Scheme 1. Scheme of the reaction network accounted by model 1 and model 2 for the HDC of 4-CP.

Fig. 1. Experimental data (symbols) and Langmuir fits (solid lines) for the adsorption equilibrium of 4-CP (a), Ph (b) and C-one (c) onto Pd/AC-AA(1) at 30 °C.

Fig. 2. Time evolution of 4-CP (▪), Ph (●) and C-one (▲) in the bulk phase with Pd/Al_2O_3 catalyst at 30 °C. Experimental (symbols) and model fit (solid lines) – model 1 (a) and model 2 (b).

Fig. 3. Time evolution of 4-CP (▪), Ph (●) and C-one (▲) in the bulk phase with Pd/AC-AA(1) at 30 °C. Experimental (symbols) and model fit (solid lines: free species, dash lines: adsorbed species) – model 1 (a) and model 2 (b).

Fig. 4. Parity plots for 4-CP (▪), Ph (◦) and C-one (▵) evolution upon HDC using model 1 (a) and model 2 (b) with Pd/Al_2O_3 (blue symbols), Pd/AC-AA(1) (black symbols), Pd/AC-SA(5) (grey symbols) and Pd/AC-AA(10) (green symbols) catalysts.

Fig. 5. Selectivity to Ph (solid lines) and C-one (dash lines) *vs.* 4-CP conversion with Pd/Al_2O_3, Pd/AC-AA(1), Pd/AC-SA(5) and Pd/AC-AA(10) catalysts at 30 °C.

Table captions

Table 1. Adsorption equilibrium data of 4-CP, Ph and C-one onto Pd/AC-AA(1), Pd/AC-SA(5) and Pd/AC-AA(10) catalysts at 30 °C.

Table 2. Values of the kinetic rate constants and pH values at the end of the reactions with the Pd/Al_2O_3 catalyst.

Table 3. Values of the kinetic rate constants obtained using model 1 and model 2, and pH values at the end of the reactions with the Pd/AC-AA(1) catalyst.

Acknowledgments

The authors gratefully acknowledge the funding of the German Research Council (DFG), which within the framework of its “Excellence Initiative” supports the Cluster of Excellence “Engineering of Advanced Materials” (www.eam.fau.de) at the University of Erlangen-Nuremberg.

References

[1] M. Pera-Titus, V. García-Molina, M.A. Baños, J. Giménez, S. Esplugas, Degradation of chlorophenols by means of advanced oxidation processes: a general review, Appl. Catal., B 47 (2004) 219-256.

[1] P. Lampi, T. Vartiainen, J. Toumisto, A. Hesso, Population exposure to chlorophenols, dibenzo-p-dioxins and dibenzofurans after prolonged ground water pollution by chlorophenols, Chemosphere 20 (1990) 625-634.

[2] M. Czaplicka, Sources and transformations of chlorophenols in the natural environment, Sci. Total Environ. 322 (2004) 21-39.

[3] Y. Persson, A. Shchukarev, L. Öberg, M. Tysklind, Dioxins, chlorophenols and other chlorinated organic pollutants in colloidal and water fractions of groundwater from a contaminated sawmill site, Environ. Sci. Pollut. Res. 15 (2008) 463-471.

[4] M.J. Gómez, S. Herrera, D. Solé, E. García-Calvo, A.R. Fernández-Alba, Automatic searching and evaluation of priority and emerging contaminants in wastewater and river water by stir bar sorptive extraction followed by comprehensive two-dimensional gas chromatography-time-of-flight mass spectrometry, Anal. Chem. 83 (2011) 2638-2647.

[5] M.A. Keane, A review of catalytic approaches to waste minimization: case study-liquid-phase catalytic treatment of chlorophenols, J. Chem. Technol. Biotechnol. 80 (2005) 1211-1222.

[6] L. Calvo, A.F. Mohedano, J.A. Casas, M.A. Gilarranz, J.J. Rodríguez, Treatment of chlorophenols-bearing wastewaters through hydrodechlorination using Pd/activated carbon catalysts, Carbon 42 (2004) 1377–1381.

[7] J.A. Baeza, L. Calvo, M.A. Gilarranz, A.F. Mohedano, J.A. Casas, J.J. Rodriguez, Catalytic behavior of size-controlled palladium nanoparticles in the hydrodechlorination of 4-chlorophenol in aqueous phase, J. Catal. 293 (2012) 85-93.

[8] M. Munoz, Z.M. de Pedro, J.A. Casas, J.J. Rodriguez, Chlorophenols breakdown by a sequential hydrodechlorination-oxidation treatment with a magnetic Pd-Fe/γ-Al_2O_3 catalyst, Water Res. 47 (2013) 3070-3080.

[9] M. Munoz, Z.M. de Pedro, J.A. Casas, J.J. Rodriguez, Combining efficiently catalytic hydrodechlorination and wet peroxide oxidation (HDC–CWPO) for the abatement of organochlorinated water pollutants, Appl. Catal., B 150–151 (2014) 197-203.

[10] C.B. Molina, A.H. Pizarro, J.A. Casas, J.J. Rodriguez, Enhanced Pd pillared clays by Rh inclusion for the catalytic hydrodechlorination of chlorophenols in water, Water Sci. Technol. 65 (2012) 653-660.

[11] M. Weber, M. Weber, M. Kleine-Boymann, Phenol, Ulmann´s Encyclopedia of Industrial Chemistry 26 (2012) 503-519.

[12] S. Kovenklioglu, Z. Cao, D. Shah, R.J. Farrauto, E.N. Balko, Direct catalytic hydrodechlorination of toxic organics in wastewater, AlChe J. 38 (1992) 1003-1012.

[13] Y. Shindler, Y. Matatov-Meytal, M. Sheintuch, Wet hydrodechlorination of *p*-chlorophenol using Pd supported on an activated carbon cloth, Ind. Eng. Chem. Res. 40 (2001) 3301-3308.

[14] E. Díaz, J.A. Casas, A.F. Mohedano, L. Calvo, M.A. Gilarranz, J.J. Rodríguez, Kinetics of the hydrodechlorination of 4-chlorophenol in water using Pd, Pt, and Rh/Al_2O_3 Catalysts, Ind. Eng. Chem. Res. 47 (2008) 3840-3846.

[15] Z.M. de Pedro, E. Diaz, A.F. Mohedano, J.A. Casas, J.J. Rodriguez, Compared activity and stability of Pd/Al_2O_3 and Pd/AC catalysts in 4-chlorophenol hydrodechlorination in different pH media, Appl. Catal., B 103 (2011) 128-135.

[16] S. Gómez-Quero, F. Cárdenas-Lizana, M.A. Keane, Liquid phase catalytic hydrodechlorination of 2,4-dichlorophenol over Pd/Al_2O_3: Batch vs. continuous operation, Chem. Eng. J. 166 (2011) 1044-1051.

[17] C.B. Molina, A.H. Pizarro, J.A. Casas, J.J. Rodriguez, Aqueous-phase hydrodechlorination of chlorophenols with pillared clays-supported Pt, Pd and Rh catalysts, Appl. Catal., B 148-149 (2014) 330-338.

[18] Y. Ukisu, S. Kameoka, T. Miyadera, Rh-Based catalysts for catalytic dechlorination of aromatic chloride at ambient temperature, Appl. Catal., B 18 (1998) 273-279.

[19] Y. Ren, G. Fan, C. Wang, Aqueous hydrodechlorination of 4-chlorophenol over an Rh/reduced graphene oxide synthesized by a facile one-pot solvothermal process under mild conditions, J. Hazard. Mater. 274 (2014) 32-40.

[20] F.J. Urbano, J.M. Marinas, Hydrogenolysis of organohalogen compounds over palladium supported catalysts, J. Mol. Catal. A: Chem. 173 (2001) 329-345.

[21] E.V. Golubina, E.S. Lokteva, S.A. Kachevsky, A.O. Turakulova, V.V. Lunin, Development and design of Pd-containing supported catalysts for hydrodechlorination, Stud. Surf. Sci. Catal. 175 (2010) 293-296.

[22] F. Alonso, I.P. Beletskaya, M. Yus, Metal-Mediated Reductive Hydrodehalogenation of Organic Halides, Chem. Rev. 102 (2010) 4009-4091.

[23] L. Calvo, M.A. Gilarranz, J.A. Casas, A.F. Mohedano, J.J. Rodríguez, Hydrodechlorination of 4-chlorophenol in aqueous phase using Pd/AC catalysts prepared with modified active carbon supports, Appl. Catal., B 67 (2006) 68-76.

[24] E. Diaz, A.F. Mohedano, J.A. Casas, L. Calvo, M.A. Gilarranz, J.J. Rodriguez, Comparison of activated carbon-supported Pd and Rh catalysts for aqueous-phase hydrodechlorination, Appl. Catal., B 106 (2011) 469-475.

[25] Y. Shao, Z. Xu, H. Wan, Y. Wan, H. Chen, S. Zheng, D. Zhu, Enhanced liquid phase catalytic hydrodechlorination of 2,4-dichlorophenol over mesoporous carbon supported Pd catalysts, Catal. Commun. 12 (2011) 1405-1409.

[26] M. Munoz, Z.M. de Pedro, J.A. Casas, J.J. Rodriguez, Improved γ-alumina-supported Pd and Rh catalysts for hydrodechlorination of chlorophenols, Appl. Catal., A 488 (2014) 78-85.

[27] J.M. Moreno, M.A. Aramendía, A. Marinas, J.M. Marinas, F.J. Urbano, Individual and competitive liquid-phase hydrodechlorination of chlorinated pyridines over alkali-modified Pd/ZrO_2, Appl. Catal., B 76 (2007) 34-41.

[28] Y. Shao, Z. Xu, H. Wan, H. Chen, F. Liu, L. Li, S. Zheng, Influence of ZrO_2 properties on catalytic hydrodechlorination of chlorobenzene over Pd/ZrO_2 catalysts, J. Hazard. Mater. 179 (2010) 135-140.

[29] C.B. Molina, L. Calvo, M.A. Gilarranz, J.A. Casas, J.J. Rodriguez, Pd–Al pillared clays as catalysts for the hydrodechlorination of 4-chlorophenol in aqueous phase, J. Hazard. Mater. 172 (2009) 214-223.

[30] A.H. Pizarro, C.B. Molina, J.A. Casas, J.J. Rodriguez, Catalytic HDC/HDN of 4-chloronitrobenzene in water under ambient-like conditions with Pd supported on pillared clay, Appl. Catal., B 158–159 (2014) 175-181.

[31] G. Yuan, M.A. Keane, Catalyst deactivation during the liquid phase hydrodechlorination of 2,4-dichlorophenol over supported Pd: influence of the support, Catal. Today 88 (2003) 27-36.

[32] Z. Jin, X. Wang, S. Wang, D. Li, G. Lu, The effect of triethylamine on the hydrodechlorination of chlorophenols on Pd/C at low temperature, Catal. Commun. 10 (2009) 2027-2030.

[33] S. Chandra Shekhar, J. Krishna Murthy, P. Kanta Rao, K.S. Rama Rao, Studies on the modifications of Pd/Al_2O_3 and Pd/C systems to design highly active catalysts for hydrodechlorination of CFC-12 to HFC-32, Appl. Catal., A 271 (2004) 95-101.

[34] F. Rodríguez-reinoso, The role of carbon materials in heterogeneous catalysis, Carbon 36 (1998) 159-175.

[35] V. Felis, C. De Bellefon, P. Fouilloux, D. Schweich, Hydrodechlorination and hydrodearomatisation of monoaromatic chlorophenols into cyclohexanol on Ru/C catalysts applied to waterdepollution: infuence of the basic solvent and kinetics of the reactions, Appl. Catal., A 20 (1999) 91-100.

[36] T.T. Bovkun, Y. Sasson, J. Blum, Conversion of chlorophenols into cyclohexane by a recyclable Pd-Rh catalyst, J. Mol. Catal. A: Chem. 242 (2005) 68-73.

[37] T. Zhou, Y. Li, T. Lim, Catalytic hydrodechlorination of chlorophenols by Pd/Fe nanoparticles: Comparisons with other bimetallic systems, kinetics and mechanism, Sep. Purif. Technol. 76 (2010) 206-214.

[38] I. Witońska, A. Królak, S. Karski, Bi modified Pd/support (SiO_2, Al_2O_3) catalysts for hydrodechlorination of 2,4-dichlorophenol, J. Mol. Catal. A: Chem. 331 (2010) 21-28.

[39] L. Calvo, M.A. Gilarranz, J.A. Casas, A.F. Mohedano, J.J. Rodriguez, Effects of support surface composition on the activity and selectivity of Pd/C catalysts in aqueous-phase hydrodechlorination reactions, Ind. Eng. Chem. Res. 44 (2005) 6661-6667.

[40] M. Streat, J.W. Patrick, M.J.C. Perez, Sorption of phenol and para-chlorophenol from water using conventional and novel activated carbons, Water Res. 29 (1995) 467-472.

[41] Q. Liu, T. Zheng, P. Wang, J. Jiang, N. Li, Adsorption isotherm, kinetic and mechanism studies of some substituted phenols on activated carbon fibers, Chem. Eng. J. 157 (2010) 348-356.

[42] B.W. Hoffer, P.H.J. Schoenmakers, P.R.M. Mooijman, G.M. Hamminga, R.J. Berger, A.D. van Langeveld, J.A. Moulijn, Mass transfer and kinetics of the three-phase hydrogenation of a dinitrile over a Raney-type nickel catalyst, Chem. Eng. Sci. 59 (2004) 259-269.

[43] C. Namasivayam, D. Kavitha, Adsorptive removal of 2-chlorophenol by low-cost coir pith carbon, J. Hazard. Mater. 98 (2003) 257-274.

[44] S. Andini, R. Cioffi, F. Montagnaro, F. Pisciotta, L. Santoro, Simultaneous adsorption of chlorophenol and heavy metal ions on organophilic bentonite, Appl. Clay. Sci. 31 (2006) 126-133.

[45] B. Özkaya, Adsorption and desorption of phenol on activated carbon and a comparison of isotherm models, J. Hazard. Mater. 129 (2006) 158-163.

Table 1

	Pd/AC-AA(1)			Pd/AC-SA(5)			Pd/AC-AA(10)		
	4-CP	Ph	C-one	4-CP	Ph	C-one	4-CP	Ph	C-one
K_{SORP} (L $mmol^{-1}$)	16.9	3.2	0.3	5.7	3.8	0.9	7.1	2.2	1.0
$C_{ADS-MAX}$ (mmol g_{cat}^{-1})	1.9	2.1	2.2	2.0	1.5	1.5	2.4	2.1	2.5
R^2	0.97	0.98	0.99	0.97	0.96	0.98	0.96	0.95	0.98

Table 2

Temperature (°C)	Model 1/Model 2		R^2	pH_{final}
	k_{HDC-1} x 10^4 (L mg_{Pd}^{-1} s^{-1})	k_{HDC-2} x 10^6 (L mg_{Pd}^{-1} s^{-1})		
20	0.85	2.69	0.98	3.5
30	1.40	4.33	0.99	3.7
40	2.31	5.90	0.99	3.8

Table 3

Temperature (°C)	Model 1		R^2	Model 2		R^2	pH_{final}
	k_{HDC-1} x 10^4 (L mg_{Pd}^{-1} s^{-1})	k_{HDC-2} x 10^6 (L mg_{Pd}^{-1} s^{-1})		k_{HDC-1} x 10^4 (L mg_{Pd}^{-1} s^{-1})	k_{HDC-2} x 10^6 (L mg_{Pd}^{-1} s^{-1})		
20	7.81	0.12	0.53	6.12	0.30	0.99	2.6
30	12.01	0.20	0.71	9.35	0.55	0.99	2.7
40	14.52	0.33	0.61	12.51	0.95	0.99	2.9

Figure 1

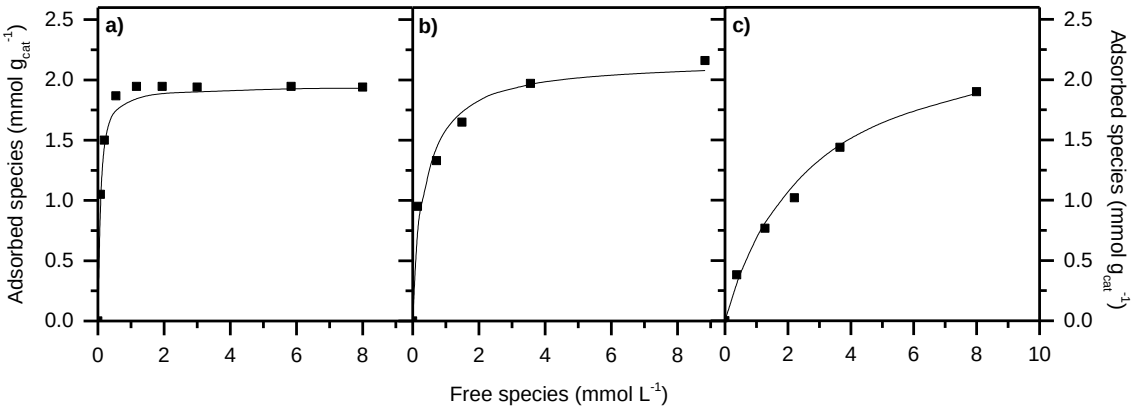

Figure 2

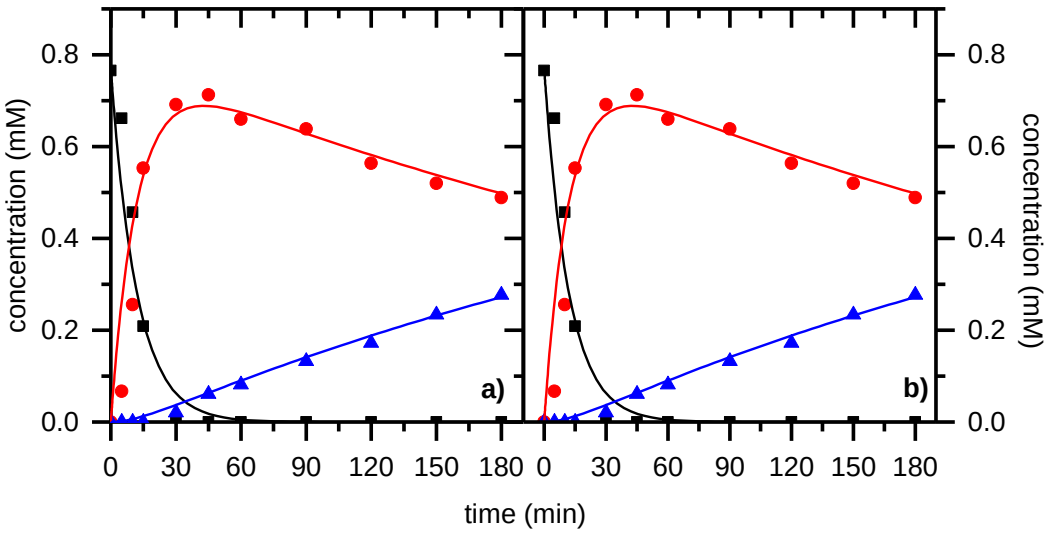

Figure 3

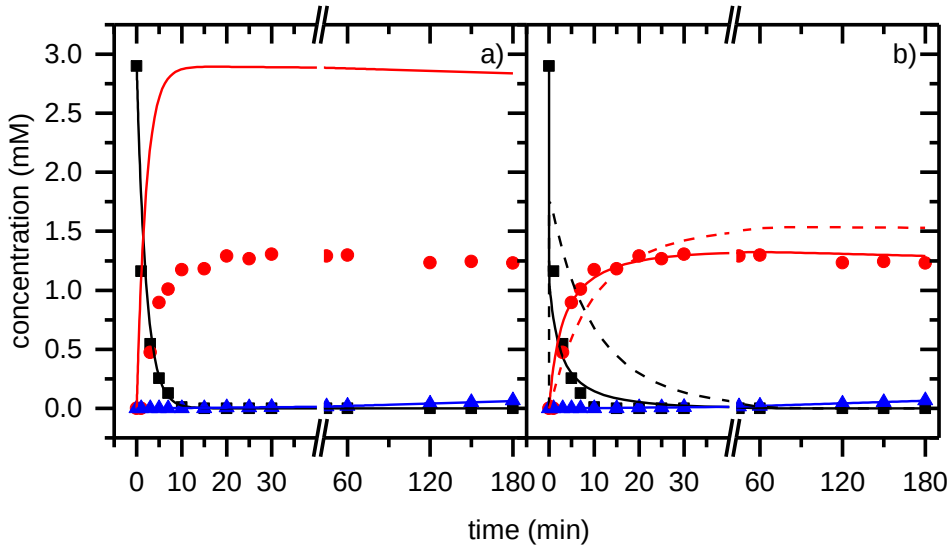

Figure 4

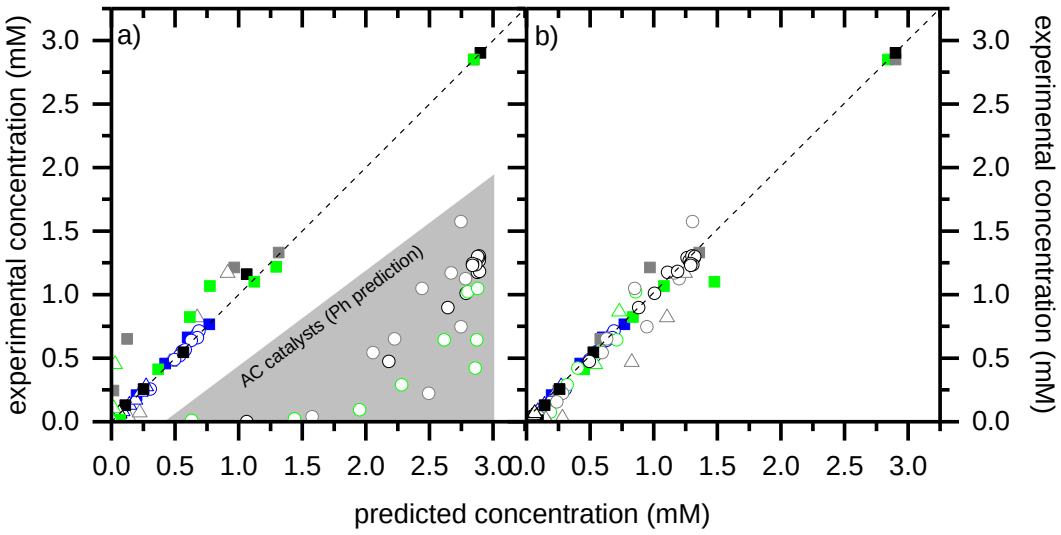

Figure 5

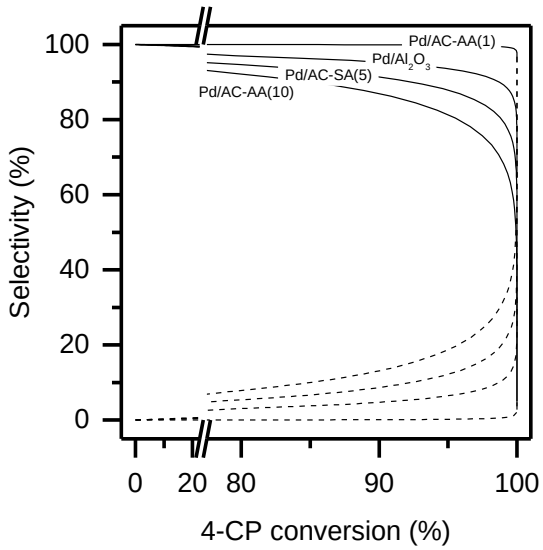

Scheme 1